

## CRIS Measurements of Electron-Capture-Decay Isotopes: $^{37}\text{Ar}$ , $^{44}\text{Ti}$ , $^{49}\text{V}$ , $^{51}\text{Cr}$ , $^{55}\text{Fe}$ , and $^{57}\text{Co}$

S. M. Niebur<sup>1</sup>, W. R. Binns<sup>1</sup>, E. R. Christian<sup>2</sup>, A. C. Cummings<sup>3</sup>, G. A. de Nolfo<sup>2</sup>, J. S. George<sup>3</sup>, P. L. Hink<sup>1</sup>, M. H. Israel<sup>1</sup>, R. A. Leske<sup>3</sup>, R. A. Mewaldt<sup>3</sup>, E. C. Stone<sup>3</sup>, T. T. von Rosenvinge<sup>2</sup>, M. E. Wiedenbeck<sup>4</sup>, and N. E. Yanasak<sup>3</sup>

<sup>1</sup>Washington University in St. Louis

<sup>2</sup>ASA/Goddard Space Flight Center

<sup>3</sup>California Institute of Technology

<sup>4</sup>Jet Propulsion Laboratory

**Abstract.** The secondary isotopes  $^{37}\text{Ar}$ ,  $^{44}\text{Ti}$ ,  $^{49}\text{V}$ ,  $^{51}\text{Cr}$ ,  $^{55}\text{Fe}$ , and  $^{57}\text{Co}$  decay only by electron capture, which occurs preferentially at the lower cosmic-ray energies, where electron attachment is more likely. Measurements of the abundances of these isotopes may reveal the interstellar energies of cosmic rays during propagation and whether reacceleration occurred. Stable secondary isotopes may also be used to examine energy dependence and reacceleration. The Cosmic Ray Isotope Spectrometer has detected large numbers of these nuclei at 100 – 500 MeV/nucleon during a time spanning solar minimum and solar maximum, allowing an additional study of solar modulation. This paper will discuss several subiron abundance ratios and the implications for reacceleration and solar modulation.

### 1 Introduction

Isotopes that decay only by electron capture,  $^{37}\text{Ar}$ ,  $^{44}\text{Ti}$ ,  $^{49}\text{V}$ ,  $^{51}\text{Cr}$ ,  $^{55}\text{Fe}$ , and  $^{57}\text{Co}$ , are generally stable at the high energies typical of cosmic rays because they are created by fragmentation of stripped cosmic rays and move at energies too high to attach an electron. For some of these isotopes, however, the electron-attachment cross sections are large enough at lower energies (where the kinetic energy of ambient electrons in the frame of the cosmic rays is comparable to the binding energy of the k-shell electrons) to allow some electron attachment and subsequent decay. The attachment cross sections decrease with energy; at the higher energies, the nuclei remain stripped and no decay occurs. These isotopes have short half-lives compared to the timescales for electron stripping and the residence time of cosmic rays in the Galaxy; if an electron becomes attached, decay will occur. The measured abundances of the electron-capture-decay isotopes at a range of energies can show whether the expected amount of decay has

occurred at each energy. Any excess decay could indicate that at one time the nuclei propagated at a lower energy, where electron attachment and decay could occur, and the cosmic rays were subsequently reaccelerated.

This technique of using secondary electron-capture-decay isotopes to probe the energy of propagating cosmic rays was originally proposed by Raisbeck *et al.* (1975), expanded by Letaw *et al.* (1984) and Silberberg and Tsao (1990), and implemented by Soutoul *et al.* (1998) using a combination of Voyager and ISEE-3 data to obtain a  $^{51}\text{V}/^{49}\text{V}$  ratio. The CRIS data set collected during the last 3.5 years is large enough to report the abundances of each of these unstable isotopes and their decay products separately, with respect to abundances of nearby stable isotopes not involved in electron-capture decay, at a range of energies. We look for consistency in the implications for reacceleration from different isotopes.

This study included the secondary electron-capture-decay isotopes  $^{37}\text{Ar}$ ,  $^{44}\text{Ti}$ ,  $^{49}\text{V}$ ,  $^{51}\text{Cr}$ ,  $^{55}\text{Fe}$ , and  $^{57}\text{Co}$  and their decay products  $^{37}\text{Cl}$ ,  $^{44}\text{Ca}$ ,  $^{49}\text{Ti}$ ,  $^{51}\text{V}$ ,  $^{55}\text{Mn}$ , and  $^{57}\text{Fe}$ . These isotopes all have half-lives of less than 2 years in the laboratory and approximately twice that with a single electron attached, as would usually be the case for a low-energy cosmic ray that picks up an electron (Wilson, 1978). We know that the measured abundances are purely secondary, for any primary abundance initially accelerated would have decayed during the  $10^5$ -year time delay prior to initial acceleration indicated by recent CRIS measurements of Ni-Co isotopes (Wiedenbeck *et al.*, 1999).

### 2 Data Analysis

The Cosmic Ray Isotope Spectrometer is one of nine instruments on the Advanced Composition Explorer (ACE), which was launched August 25, 1997. CRIS detects He-Zn nuclei of 50 – 550 MeV/nucleon at 1 AU; the isotopes discussed in this paper were measured at energies of 100 – 500 MeV/nucleon. CRIS has a large collecting power

(geometrical factor of  $250 \text{ cm}^2\text{sr}$ ), and has therefore collected a large number of events, which allows division of the data into several energy bins and subsequent examination of possible energy dependence of isotopic abundance ratios. The mass resolution of the binned data is  $\leq 0.25 \text{ amu}$ ; the peaks are clearly separated (Niebur *et al.*, 2000). The instrument is more fully described in Stone *et al.* (1998).

The data discussed in the next two sections were collected during solar minimum (August 28, 1997 – August 17, 1999); the data in the last section were collected during solar maximum (July 25, 2000 – April 20, 2001). The data were divided into energy bins, and the mass histograms were fit using a multiple Gaussian fitting routine. The resulting isotopic abundances were converted to ratios and corrected to compensate for fragmentation in the instrument and differences in spectral shape. The data were compared to results from a leaky-box propagation model (Leske, 1993) modified as described in Davis *et al.* (2000). The model uses electron-attachment cross sections calculated as in Crawford (1979) and escape pathlength in the Soutoul and Pustkin (1999) formulation with parameters adjusted to fit the measured subiron abundances.

In each of the following plots, the solid line shows the results of the standard leaky-box model and the dashed line shows results of the same model with electron attachment turned off, to emphasize the effects of electron attachment on the model results. A one-dimensional Fisk solar modulation model (Fisk, 1971) was applied to the data after the propagations, using a solar modulation level of  $\phi=350 \text{ MV}$  at solar minimum and  $\phi=1075 \text{ MV}$  at solar maximum.

### 3 Results: Electron-capture-decay isotopes

The electron-capture-decay isotopes  $^{49}\text{V}$  and  $^{51}\text{Cr}$  show electron-capture decay at the lower energies measured by CRIS. At the lower energies, the data show an enhancement of the decay products ( $^{49}\text{Ti}$  and  $^{51}\text{V}$ ), as predicted by the leaky-box propagation model that allowed electron capture decay (solid lines in Figure 1). The abundances of the unstable isotopes themselves are

correspondingly depleted, consistent with electron capture decay. In each case, the unstable isotope or product is shown relative to nearby stable isotope(s)  $^{46}\text{Ti}+^{47}\text{Ti}+^{48}\text{Ti}$  or  $^{52}\text{Cr}$ .

Both sets of isotopes, as well as the other secondary electron-capture-decay isotope pairs  $^{37}\text{Ar}/^{37}\text{Cl}$ ,  $^{44}\text{Ti}/^{44}\text{Ca}$ ,  $^{55}\text{Fe}/^{55}\text{Mn}$ , and  $^{57}\text{Co}/^{57}\text{Fe}$ , show good qualitative agreement of the data with the leaky-box propagation model that incorporates electron-capture decay. However, the  $^{49}\text{Ti}/(^{46}\text{Ti}+^{47}\text{Ti}+^{48}\text{Ti})$  data points in Figure 1 lie to the left of the propagation curve, and the  $^{51}\text{V}/^{52}\text{Cr}$  data points lie slightly to the right of the propagation curve for that ratio. If the data points for the two isotope pairs (and the others) fell consistently on the right side of the curve (like  $^{51}\text{V}/^{52}\text{Cr}$ ), we could conclude that reacceleration may have occurred, shifting the measured ratios to higher energies than expected by the model. If instead all the data points fell to the left of the curves (like  $^{49}\text{Ti}/(^{46}\text{Ti}+^{47}\text{Ti}+^{48}\text{Ti})$ ), the discrepancy could be explained by an incorrect level of solar modulation and resolved using a higher solar modulation level in the model. The first case could also be explained by an incorrect level of solar modulation and resolved by reducing the solar modulation level. In that scenario, it would be extremely difficult to separate the effects of reacceleration and solar modulation, as the absolute level of solar modulation at any given time is not well-known and incorrect levels of solar modulation can produce similar effects as reacceleration.

Since we are able to compare the data and model results for several isotope pairs and they do not show a consistent result, no conclusion about reacceleration or solar modulation can be made from the electron-capture-decay isotopes alone. Instead, some other energy-dependent parameter, such as incorrect nuclear fragmentation cross sections, may cause the offset. The fragmentation cross sections for the subiron elements in this energy range (500 – 1000 MeV/nucleon) have not been completely measured; the cross sections used in the model are based on the semi-empirical formulations of Silberberg, Tsao, and Barghouty (1998), with corrections for isotopes where measurements exist (Webber, Kish, and Schrier, 1990; Knott *et al.*, 1997; Chen *et al.*, 1997a, 1997b; Vonach *et al.*, 1997; Webber

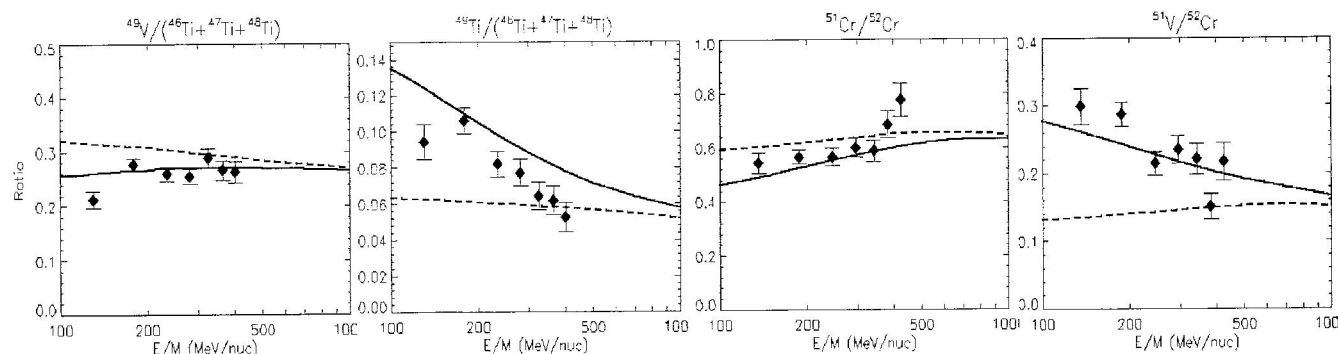


**FIGURE 1.** Parent and daughter abundances for the electron-capture-decay isotopes  $^{49}\text{V}$  and  $^{51}\text{Cr}$  and their decay products  $^{49}\text{Ti}$  and  $^{51}\text{V}$ , relative to nearby stable isotope(s)  $^{46}\text{Ti}+^{47}\text{Ti}+^{48}\text{Ti}$  and  $^{52}\text{Cr}$ , respectively. Plotted curves are leaky-box propagation model results, with (solid) and without (dashed) electron-capture decay. Reacceleration is not included in this modeling calculation.

*et al.*, 1998a, 1998b). A new set of nuclear fragmentation cross sections for production of all isotopes involved would shift several propagation curves accordingly and may result in better agreement between data and model (George *et al.*, 2001). The other electron-capture-decay isotope pairs,  $^{37}\text{Ar}/^{37}\text{Cl}$ ,  $^{44}\text{Ti}/^{44}\text{Ca}$ ,  $^{55}\text{Fe}/^{55}\text{Mn}$ , and  $^{57}\text{Co}/^{57}\text{Fe}$ , are not useful for this study, as the magnitude of difference between the models with and without electron capture in the measured energy range is smaller than the uncertainties on the data. The abundances of these isotopes and selected ratios can be found in Niebur (2001).

#### 4 Results: Stable secondary isotopes

In the previous section, electron-capture-decay isotopes were used as an energy marker to determine whether the nuclei once propagated at a different energy than the energy at which they enter the heliosphere. There is another technique that can be used to probe whether the cosmic rays have encountered interstellar shocks and been reaccelerated in the interstellar medium. This method for discriminating between distributed acceleration models and direct acceleration (e.g. standard leaky-box) models was formally proposed by Giler, Wdowczyk, and Wolfendale (1988), who advocated exploiting the energy dependence of nuclear fragmentation cross sections by comparing ratios of fragmentation products. The secondary  $^{56}\text{Fe}$  ratios that show energy dependence can also serve as an energy marker. Two examples,  $(^{42}\text{Ca}+^{43}\text{Ca})/^{56}\text{Fe}$  and  $^{46}\text{Ti}/^{56}\text{Fe}$ , are shown in Figure 2.

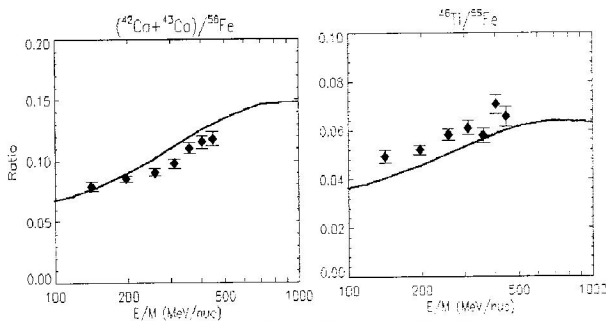


**FIGURE 2.** The  $(^{42}\text{Ca}+^{43}\text{Ca})/^{56}\text{Fe}$  and  $^{46}\text{Ti}/^{56}\text{Fe}$  ratios at solar minimum as a function of energy. These stable secondary  $^{56}\text{Fe}$  ratios show energy dependence over the measured energy range due to the energy-dependent  $^{56}\text{Fe}$  fragmentation cross sections.

These plots show the same inconsistency in the data-model comparisons as the electron-capture-decay isotopes did in the previous section. The  $(^{42}\text{Ca}+^{43}\text{Ca})/^{56}\text{Fe}$  data fall to the right of the propagation curve, while the  $^{46}\text{Ti}/^{56}\text{Fe}$  data points fall to the left of the corresponding propagation curve. No consistent explanation can be found using reacceleration or solar modulation alone; the new nuclear fragmentation cross section measurements from George *et al.* (2001) should be incorporated into the propagation model and the results re-examined.

#### 5 Solar modulation

As mentioned in the previous sections, it is extremely difficult to separate the possible effects of reacceleration and solar modulation in a single data set. However, CRIS has now collected data through the most recent solar minimum and the current solar maximum. Comparison of data collected during each of these time periods may provide a clear demonstration of the effects of solar modulation. In Figure 3, the data collected at solar minimum (solid diamonds) are from the same data set as the data shown in Figure 1. The data collected at solar maximum (open squares) were divided into fewer energy bins, as the number of particles collected is much smaller, due to the shorter time period of collection to date and the substantial decrease in the flux of the galactic cosmic rays at solar maximum. The solid lines in Figure 3 represent the results of the leaky-box propagation model with electron attachment at solar minimum.

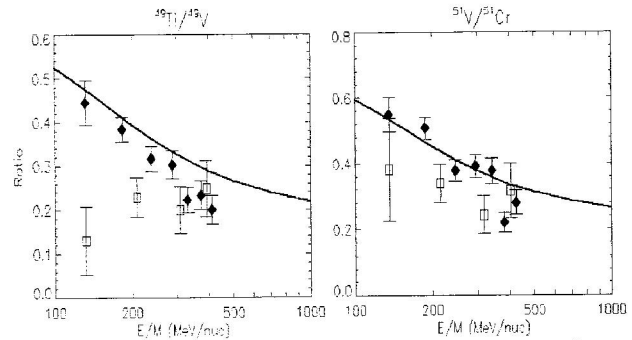


**FIGURE 3.** Electron-capture-decay isotope ratios  $^{49}\text{Ti}/^{49}\text{V}$  and  $^{51}\text{V}/^{51}\text{Cr}$  measured at solar minimum (diamonds) and solar maximum (squares) have distinctly different values. The values measured at solar maximum are approximately the same as the values for the highest-energy measurements during solar minimum, demonstrating that higher levels of solar modulation involve higher levels of energy loss.

Although the electron-capture-decay isotopes collected at solar minimum show energy-dependent electron-capture decay over this energy range, the ones collected at solar maximum do not. In fact, over the entire observed energy range, the solar maximum ratios are similar to those seen at the highest energies during solar minimum. A simple calculation of the difference in solar modulation using the force-field approximation yields a difference in rigidity of  $\phi \sim 725$  MV, or  $\Phi \sim 365$  MeV/nucleon for these isotopes with  $A/Z \sim 2$ . Therefore, the nuclei collected during solar maximum entered the heliosphere a few hundred MeV/nucleon higher (on average) in energy than those collected during solar minimum and the lowest energy particles at solar maximum correspond roughly to the highest energy particles collected at solar minimum. The similarity of the solar minimum data at the highest energies and the solar maximum data at even the lowest energies is not surprising, assuming that solar modulation includes energy loss, as has been long assumed and incorporated into the models (e.g. Goldstein, Fisk, and Ramaty, 1970). These

data provide a direct demonstration that solar modulation does include energy loss.

## 6 Conclusions

The ACE-CRIS instrument has produced evidence of energy-dependent electron-capture decay in qualitative agreement with our leaky-box propagation model. However, these data do not yet permit a clear conclusion about reacceleration in the interstellar medium. While comparison of  $^{51}\text{V}/^{52}\text{Cr}$  data with calculations assuming no reacceleration shows a discrepancy that could be explained by reacceleration, the comparison of  $^{49}\text{Ti}/(^{46}\text{Ti}+^{47}\text{Ti}+^{48}\text{Ti})$  data with calculations suggest the opposite conclusion. Nearby stable isotope ratios ( $^{42}\text{Ca}+^{43}\text{Ca}/^{56}\text{Fe}$  and  $^{46}\text{Ti}/^{56}\text{Fe}$ ) show similar effects, which cannot be sufficiently explained by reacceleration or incorrect levels of solar modulation. These discrepancies suggest problems with the nuclear fragmentation cross sections used in the calculations. We expect that newly measured cross sections, now being analyzed (George *et al.*, 2001), may resolve the discrepancies.

A comparison of the data collected at solar minimum and solar maximum shows that the energy dependence observed at solar minimum is not apparent at solar maximum. All the solar-maximum values tend to cluster near the values of the highest energy measurements at solar minimum. This result is a direct confirmation that increasing levels of solar modulation involve increased amounts of energy loss as interstellar cosmic rays approach the inner solar system.

*Acknowledgements.* This research was supported by the National Aeronautics and Space Administration at the California Institute of Technology (under grant NAG5-6912), the Goddard Space Flight Center, the Jet Propulsion Laboratory, and Washington University in St. Louis. One of us (S.M.N.) also wishes to acknowledge the support of the Mr. and Mrs. Spencer T. Olin Foundation.

## References

- Chen, C.-X. *et al.* (1997a) *Astrophys. J.* 479:504-521.  
 Chen, C.-X. *et al.* (1997b) *Phys. Rev. C* 56:1536-1543.  
 Crawford, H.J. (1979) Ph.D. Thesis. University of California at Berkeley. LBL-8807.  
 Davis, A.D. *et al.* (2000) In R.A. Mewaldt *et al.* (eds.), *Acceleration and Transport of Energetic Particles Observed in the Heliosphere*, New York, pp. 421-424.  
 Fisk, L.A. (1971) Solar modulation of galactic cosmic rays, 2. *J. Geophys. Res.* 76:221-226.  
 George, J.S. *et al.* (2001) These proceedings.  
 Giler, M., Wdowczyk, J., and Wofendale, A. W. (1988) *Astron. Astrophys.* 196:4-48.  
 Goldstein, M.L., Fisk, L. A., and Ramaty, R. (1970) *Phys. Rev. Lett.* 25:832-835.  
 Knott, C.N. *et al.* (1997) *Phys. Rev. C* 56:398-406.  
 Leske, R.A. (1993) *Astrophys. J.* 405:567-583.

- Letaw, J. R., Silberberg, R., and Tsao, C. H. (1984) *Astrophys. J. Supp.* 56:369-391.  
 Niebur, S.M. (2001) Ph.D. thesis. Washington University in St. Louis.  
 Niebur, S.M. *et al.* (2000) In R.A. Mewaldt *et al.* (eds.), *Acceleration and Transport of Energetic Particles Observed in the Heliosphere*, New York, pp. 406-409.  
 Raisbeck, G.M. *et al.* (1975) *Proc. 14<sup>th</sup> Internat. Cosmic Ray Conf.* 2:560-563.  
 Silberberg, R., Tsao, C. H., and Barghouty, A. F. (1998) *Astrophys. J.* 501:911-919.  
 Silberberg, R. *et al.* (1983) *Phys. Rev. Lett.* 51:1217-1220.  
 Silberberg, R. and Tsao, C. H. (1990) *Phys. Reports* 191:351-408.  
 Soutoul, A. *et al.* (1998) *Astron. Astrophys.* 336:L61-L64.  
 Soutoul, A., and Ptuskin, V.S. (1999) *Proc. 26<sup>th</sup> Internat. Cosmic Ray Conf.* 4:184-186.  
 Stone, E.C. *et al.* (1998) *Space Sci. Rev.* 88:285-356.  
 Vonach, H. *et al.* (1997) *Phys Rev C* 55:2458-2467.  
 Webber, W. R. *et al.* (1998a) *Astrophys. J.* 508:949-958.  
 Webber, W. R. *et al.* (1998b) *Phys. Rev. C.* 58:3539-3552.  
 Webber, W.R., Kish, J.C., and Schrier, D.A. (1990) *Phys. Rev. C* 41:547-565.  
 Wiedenbeck, M. E. *et al.* (1999) *Astrophys. J.* 523:L61-L64.  
 Wilson, L.W. (1978) Ph.D. thesis. University of California at Berkeley. LBL-7723.